NASA
Technical Memorandum 82840

AVRADCOM
Technical Report 82-C-5

Tooth Profile Analysis of Circular-Cut, Spiral-Bevel Gears

Ronald L. Huston
University of Cincinnati
Cincinnati, Ohio

and

Yael Lin
Technion—Israel Institute of Technology
Haifa, Israel

and

John J. Coy
Propulsion Laboratory
AVRADCOM Research and Technology Laboratories
Lewis Research Center
Cleveland, Ohio

Prepared for the
Design Engineering Technical Conference
sponsored by the American Society of Mechanical Engineers
Washington, D.C., September 12–15, 1982

NASA

U.S. ARMY AVRADCOM

TOOTH PROFILE ANALYSIS OF CIRCULAR-CUT, SPIRAL-BEVEL GEARS

Ronald L. Huston*
University of Cincinnati
Cincinnati, Ohio 45221

Yael Lin
Technion - Israel Institute of Technology
Haifa 32000, Israel

John J. Coy*
Propulsion Laboratory
AVRADCOM Research and Technology Laboratories
NASA Lewis Research Center
Cleveland, Ohio 44135

ABSTRACT

An analysis of tooth profile changes in the transverse plane of circular-cut, spiral-bevel crown gears is presented. The analysis assumes a straight-line profile in the midtransverse plane. The profile variation along the centerline is determined by using expressions for the variation of the spiral angle along the tooth centerline, together with the profile description at the midtransverse plane. It is shown that the tooth surface is a hyperboloid and that significant variations in the pressure angle are possible.

INTRODUCTION

This paper presents an analysis of tooth profile changes, heel to toe, of circular-cut, spiral-bevel crown gears. These changes are examined in the transverse plane of the gear.

Recently, there has been increased interest in determining the effects of slight profile changes on the kinematics, noise, stress analysis, wear, and life of spiral-bevel gears. This interest has been stimulated by a desire to improve operating and maintenance procedures in high-performance transmissions of helicopters and other aircraft. References [1-6][1] are examples of recent approaches taken to develop a broader understanding of the geometrical characteristics of spiral-bevel and hypoid gears. It is believed that a quantitative understanding of the geometrical characteristics is fundamental to analyses of the above-mentined physical phenomena of these gears.

Spiral-bevel gears are used in high-performance transmissions because their curved teeth provide smoother and quieter operation than straight-bevel gear teeth. Also, the curved teeth provide greater bending resistance. Figure 1 shows a spiral-bevel gear and its pinion.

*Member ASME.

[1]Numbers in brackets refer to references listed at the end of the paper.

These gears are called "spiral"-bevel gears since the theoretical centerline of the gear tooth is a logarithmic spiral [7]. A logarithmic spiral has the advantage of providing equal angles between the tooth centerline and radial lines, at all points along the centerline. This in turn provides uniform geometical characteristics of the tooth profile in the transverse planes of the gear, that is, the planes normal to the radial pitch lines of the gear. However, the disadvantages of logarithmic spiral teeth are that they are difficult to fabricate and the tooth surface itself is often considered to be too "flat" to incorporate the advantages of curved teeth [8]. Therefore, most gear manufacturers have been cutting spiral-bevel gears with circular cutters.

The advantages of circular cutters are that they are relatively easy to use in manufacturing processes and that, through varying the cutter radius and the position of the cutter center, a variety of toothforms can be produced. Also, for a carefully chosen cutter setting and cutter radius a circular cut can very nearly approximate a logarithmic spiral [7]. The disadvantage of circular cutters is that the uniform tooth profile in the transverse plane is lost, leading to distortions along the centerline. It is the objective of this paper to investigate these distortions.

The analysis of the paper is performed on crown gears with straight profiles in the midtransverse plane. A crown gear (sometimes called a crown rack) is a flat gear and is thus analogous to a rack for spur gears. Many spiral-bevel gears have apex angles that are nearly 90° and are thus approximately crown gears (fig. 1). Also, the analysis is developed in the transverse planes since, as mentioned previously, these planes are normal to the radial pitch lines of the gear. The transverse planes are thus the planes of the transmitted force vector from the pinion to the gear. Moreover, the transverse planes are perpendicular to both the pitch and axial planes of the gear and they are tangent to the theoretical "bevel gear sphere" [9] with center at the gear apex.

SYMBOLS

C	cutter center
H	horizontal cutter setting
k	cotangent of pressure angle
$\underset{\sim}{n}_r$	radial unit vector
$\underset{\sim}{n}_\theta$	transverse unit vector
P	typical point on gear centerline
P_m	midpoint on tooth centerline
$\underset{\sim}{p}$	position vector to typical point on curve

O	gear center
R_c	cutter radius
R_i	inside radial distance
R_m	mean radial distance
R_o	outside radial distance
r	radial coordinate from O
$\hat{r}$	radial coordinate from C
t_o	transverse tooth thickness
V	vertical cutter setting
X,Y,Z	coordinate axes with origin at O and with X-Y plane coincident with pitch plane
$\hat{X},\hat{Y},\hat{Z}$	coordinate axes with origin at C and with X-Y plane coincident with pitch plane
x,y,z	distance relative to X,Y,Z coordinate system
$\hat{x},\hat{y},\hat{z}$	distance relative to $\hat{X},\hat{Y},\hat{Z}$ coordinate system
γ	angle OPC in fig. 5
θ	pressure angle in transverse plane
ρ	radius of curvature
φ	transverse angle
φ_m	midtransverse angle
ψ	spiral angle
ψ_m	midspiral angle
$\Delta\psi$	spiral-angle change ($\psi - \psi_m$)

PRELIMINARY CONSIDERATIONS

Configuration

Figure 2 depicts a top view of some of the geometrical features of a circular-cut crown gear, which will be useful in the following analysis. Specifically, O is the gear center or "gear apex" and C is the circular cutter center with a cutter radius R_c in the pitch (X-Y) plane. The spiral angle ψ is the angle between a radial line through O and the

tooth centerline. The midspiral angle ψ_m, shown in figure 2, is the angle between the tooth centerline and the radial line passing through the midpoint of the tooth centerline (the X-axis). Finally, figure 2 has two sets of coordinate axes X,Y,Z and $\hat{X},\hat{Y},\hat{Z}$ with origins at O and C, respectively. The coordinates are then related by the simple expressions

$$\hat{x} = x - H, \qquad \hat{y} = y - V, \qquad \hat{z} = z \tag{1}$$

where H and V are the horizontal and vertical cutter center settings.

Spiral Angles

The spiral angle ψ varies along the centerline of the tooth. For example, figure 3 shows a series of radial lines intersecting the tooth centerline. It is easily seen that the spiral angles are all distinct; that is,

$$\psi_1 \neq \psi_2 \neq \psi_m \neq \psi_3 \neq \psi_4 \tag{2}$$

Figure 3 also shows transverse lines (edge views of transverse planes) intersecting the tooth centerline and forming "transverse angles" φ, which are complements of the spiral angles. The transverse angles are also distinct; that is,

$$\varphi_1 \neq \varphi_2 \neq \varphi_m \neq \varphi_3 \neq \varphi_4 \tag{3}$$

Interestingly, if the tooth centerline is a logarithmic spiral, the spiral angles are all equal; that is,

$$\psi_1 = \psi_2 = \psi_m = \psi_3 = \psi_4 \tag{4}$$

Similarly, the transverse angles are also all equal for a logarithmic spiral tooth centerline; that is,

$$\varphi_1 = \varphi_2 = \varphi_m = \varphi_3 = \varphi_4 \tag{5}$$

Logarithmic Spiral and Circular Arc

The property described by equations (4) and (5) is an attractive feature of logarithmic spiral tooth centerlines. Indeed, for such a centerline the tooth profiles, obtained by the intersection of the tooth surface and the transverse planes, are all similar.

A logarithmic spiral has an equation of the form

$$r = R_m e^{m\theta} \tag{6}$$

where r and θ are the radial and transverse (polar) coordinates of a typical point P on the curve. For a logarithmic spiral tooth centerline, R_m is the distance from O to P_m, the midpoint on the tooth centerline, and m is the cotangent of the spiral angle. That is,

$$m = \cot \psi \tag{7}$$

(Eq. (7) follows from eq. (6) by noting that $dr/d\theta = mr$ and that when $\theta = 0$ the slope is $\tan \psi = \tan \psi_m = r\, d\theta/dr$.)

Buckingham [7] has shown that there is very little difference between a logarithmic spiral tooth centerline and a circular arc if the radius R_c of the circular arc is the same as the radius of curvature at the midpoint P_m of the logarithmic spiral. It is easily seen (appendix A) that the radius of curvature of a logarithmic spiral of the form of equation (6) is

$$\rho = r(1 + m^2)^{1/2} = r/\sin \psi \tag{8}$$

where the second equality follows from using equation (7). Hence, a nearly coincident circle is obtained by letting R_c be

$$R_c = R_m/\sin \psi_m \tag{9}$$

From figure 2 the horizontal and vertical cutter settings are then

$$H = R_m - R_c \sin \psi_m = 0 \tag{10}$$

and

$$V = R_c \cos \psi_m = R_m \cot \psi_m \tag{11}$$

For a typical midspiral angle of 30°, equations (9) and (10) show that the cutter radius would be twice the mean gear radius and that the cutter center would be on the Y-axis. This is sometimes considered to be impractical for fabrication [7]. Moreover, the tooth shape is often deemed to be "too flat" [8]. Nevertheless, for a gear with a mean radius of 177.8 mm (7.0 in.) Buckingham has shown (see also eq. (14) below) that the difference in spiral angles between the circular arc and the logarithmic spiral tooth centerline at the heel and toe is less than 1/2°. A computer plot comparing a circular arc with a logarithmic spiral tooth centerline for a more realistic cutter setting and radius is shown in figure 4. In this figure the mean radius R_m is again 177.8 mm (7.0 in.) and the midspiral angle is 30°, but the cutter radius R_c is reduced to 152.4 mm (6.0 in.). Equations (10) and (11) then give the horizontal and vertical cutter settings to be H = 101.6 mm (4.0 in.) and V = 132.98 mm ($3\sqrt{3}$ in.) In this case, the spiral angles differ by approximately 6° at the heel and toe.

Variation of Spiral Angle Along Circular-Cut Tooth Centerline

It is helpful to develop an expression for the change in the spiral angle along a circular-arc tooth centerline. Such an expression is easily obtained from figure 5, which shows an enlarged (but not to scale) view of the circular-arc tooth. Then, using the law of cosines with triangle OPC leads immediately to the expression

$$(\overline{OC})^2 = (\overline{OP})^2 + (\overline{CP})^2 - 2(\overline{OP})(\overline{CP})\cos\gamma \tag{12}$$

By recognizing that $\cos\gamma = \sin\psi$, $(\overline{OC})^2 = H^2 + V^2$, $(\overline{OP})^2 = r^2$, and $(\overline{CP})^2 = R_c^2$, equation (12) can be rewritten in the form

$$H^2 + V^2 = r^2 + R_c^2 - 2rR_c \sin\psi$$

or as

$$\sin\psi = (r^2 + R_c^2 - H^2 - V^2)/2rR_c \tag{13}$$

Finally, by noting in figure 5 that $H = R_m - \frac{}{2} R_c \sin\psi_m$ and $V = R_c \cos\psi_m$ (eqs. (10) and (11)), equation (13) becomes[2]

$$\sin\psi = (r^2 - R_m^2 + 2R_mR_c \sin\psi_m)/2rR_c \tag{14}$$

ANALYSIS

Determination of Effect of Spiral Angle Changes on Traverse Tooth Profile

Consider again the change in the transverse angle φ as shown in figure 3 and recorded by equation (3). These changes can be simulated by cutting a circle with radius R_c by vertical lines at varying dixtances x from the origin, as shown in figure 6. (Alternatively, fig. 6 may be viewed as representing transverse cutting planes passing through a surface of revolution.) Then it is immediately seen that

$$x = R_c \cos\varphi = R_c \sin\psi \tag{15}$$

This relatively simple result is an effective algorithm for studying tooth profiles in the transverse plane; that is, the transverse tooth profile for any spiral angle ψ can be obtained by passing a cutting plane through the circular-cut tooth surface of revolution at a distance x from the cutter axis, where x is given by equation (15).

[2]This expression is identical to that recorded by Baxter [9].

Determination of Form of Surface of Revolution for Straight-Line Profile in Transverse Plane

If a crown gear has a straight-line profile in the transverse plane, it is analogous to the involute rack of spur gears. Such a gear is sometimes called a "crown rack" [7]. Consider figure 7, which shows the pitch plane of a crown gear together with a typical tooth centerline and the coordinate axes. Imagine a transverse plane cutting the tooth surface and passing through the midpoint of the tooth centerline as shown. Then, if the crown gear is to simulate a crown rack at its midpoint, the tooth profile in the midtransverse plane might appear as shown in figure 8.

The equations of the left and right sides of the tooth surface in this midtransverse plane are then of the form

$$z = k(y + t_0/2) \tag{16}$$

and

$$z = -k(y - t_0/2) \tag{17}$$

where t_0 is the transverse tooth thickness in the pitch plane and k is the cotangent of the pressure angle θ; that is,

$$k = \cot \theta \tag{18}$$

The equation of the tooth surface of revolution generated by the circular cutter can be expressed in the form

$$\hat{z} = f(\hat{r}) \tag{19}$$

were $\hat{r}$, the radial distance from the cutter center C, is

$$\hat{r} = (\hat{x}^2 + \hat{y}^2)^{1/2} \tag{20}$$

The equation of the midtransverse cutting plane as shown in figure 7 is simply

$$\hat{x} = R_c \sin \psi_m \tag{21}$$

When $\hat{x}$ has the value $R_c \sin \psi_m$, $f(\hat{r})$ as determined by equations (20) and (21) has the form of equations (16) or (17) for a straight-line profile in the midtransverse plane. Substituting from equation (21) into (20) and then into (19) and solving for $\hat{y}$ lead to

$$\hat{y} = -(\hat{r}^2 - R_c^2 \sin^2 \psi_m)^{1/2} \tag{22}$$

where the negative root is taken since $\hat{y}$ is negative (fig. 7). Hence, from equations (1) and (16) to (19), $f(\hat{r})$ takes the form

$$f(\hat{r}) = [V + (t_0/2) - (\hat{r}^2 - R_c^2 \sin^2\psi_m)^{1/2}]\cot\theta \tag{23}$$

or

$$f(\hat{r}) = [-V + (t_0/2) + (\hat{r}^2 \quad R_c^2 \sin^2\psi_m)^{1/2}]\cot\theta \tag{24}$$

where equation (23) corresponds to the left or "outside" tooth surface and equation (24) corresponds to the right or "inside" tooth surface. It is easily shown that these surfaces of revolution are hyperboloids (appendix B).

APPLICATION - NUMERICAL RESULTS

Approximate Analysis

In equations (23) and (24), if $\hat{x} = R_c \sin\psi_m$ in $\hat{r}$, then $f(\hat{r})$ becomes $[V + (t_0/2) + \hat{y}]\cot\theta$ or $[-V + (t_0/2) - \hat{y}]\cot\theta$ depending on whether $f(\hat{r})$ describes an "outside" or "inside" tooth surface. As expected, these expressions match those of the straight-line profiles of equations (16) and (17). (These are, of course, the tooth profiles in the midtransverse plane.) If, however, in equations (23) and (24), $\hat{x} = R_c \sin\psi$, that is, if $\psi \neq \psi_m$, the transverse tooth profiles are no longer straight but instead are described by the expressions

$$z = [V + (t_0/2) - (R_c^2 \sin^2\psi + \hat{y}^2 - R_c^2 \sin^2\psi_m)^{1/2}]\cot\theta \tag{25}$$

and

$$z = [-V + (t_0/2) + (R_c^2 \sin^2\psi + \hat{y}^2 - R_c^2 \sin^2\psi_m)^{1/2}]\cot\theta \tag{26}$$

From figure 4 and from an examination of equation (14) it is evident that there is relatively little numerical difference between the spiral angle ψ and the midspiral angle ψ_m. Hence, by letting $\Delta\psi$ be the difference $\psi - \psi_m$, it is reasonable to make approximations in equations (25) and (26) by neglecting powers of $\Delta\psi$. By noting that $\sin^2\psi - \sin^2\psi_m = 1/2(\cos 2\psi_m - \cos\psi) \approx \Delta\psi \sin 2\psi_m$, by using the binomial expansion, and by recalling that $\hat{y}$ is negative, equations (25) and (26) can be expressed as

$$z = [V + (t_0/2) + \hat{y} + (R_c^2/\hat{y})\Delta\psi \sin\psi_m \cos\psi_m]\cot\theta \tag{27}$$

and

$$z \approx [-V + (t_0/2) - \hat{y} - (R_c^2/y)\Delta\psi \sin \psi_m \cos \psi_m]\cot \theta \qquad (28)$$

Equations (27) and (28) when used in conjunction with equations (16) and (17) are a measure of the transverse tooth profile change in terms of the spiral angle change $\Delta\psi$ along the tooth centerline.

Exact Analysis

Equations (25) and (26) can also be used to obtain an exact or numerical analysis of the transverse tooth profile change along the centerline. That is, by using equation (13) or (14) the variation of z with y (transverse distance) and with r (radial distance) is determined if the cutter settings and cutter radius are known.

Such numerical calculations were performed for a crown gear with a cutter radius R_c of 152.4 mm (6.0 in.), horizontal and vertical cutter settings H and V of 101.6 mm (4.0 in.) and 131.98 ($3\sqrt{3}$ in.), a midspiral angle ψ_m of 30°, and a pressure angle θ_m at the midtransverse plane of 20°. Also, the inner and outer gear radii were taken as 152.4 and 203.2 mm (6.0 and 8.0 in.), respectively. (The data are also the same as those used in the gear depicted in fig. 4.)

These calculations were performed for the left or "outside" tooth surface. The results are shown in figures 9 to 12, where the pressure angle is plotted as a function of the radial distance r, the vertical coordinate z, and the transverse coordinate y.

CONCLUSIONS

Perhaps the most interesting of the results are the curves showing the variation of the pressure angle along the radius for different elevations in the tooth profile. Changes in the pressure angle can, of course, affect the stress distribution on the surface and on the rest of the tooth, as well as the kinematics and possibly the conjugate action. Moreover, it appears that these effects are likely to be enhanced in noncrown or conical gears.

The results also show (eqs. (25) and (26)) that the transverse tooth profile will not be straight except in the midtransverse plane. This could also affect the stress distribution and surface kinematics.

Finally, the procedure outlined in equations (16) to (23) for determining the cutter profile can be used for any desired tooth profile shape. Also, the effect of the spiral-angle change on such tooth shapes in the transverse plane can be determined by following the procedure outlined in equations (27) and (28).

APPENDIX A

RADIUS OF CURVATURE OF A LOGARITHMIC SPIRAL

The radius of curvature of a curve can be expressed in the form [10]

$$\rho = \left|\underset{\sim}{dp/d\theta}\right|^3 \Big/ \left|(\underset{\sim}{dp/d\theta}) \times (\underset{\sim}{d^2p/d\theta^2})\right| \qquad \text{(A1)}$$

where p is the position vector to a typical point on the curve and θ is a parameter defining the locus of the points on the curve. For the plane tooth centerline in the form of the logarithmic spiral of equation (7), $\underset{\sim}{p}$ can be expressed as

$$\underset{\sim}{p} = r\underset{\sim}{n}_r = R_m e^{m\theta}\underset{\sim}{n}_r \qquad \text{(A2)}$$

where $\underset{\sim}{n}_r$ is a radial unit vector. If $\underset{\sim}{n}_\theta$ is a transverse unit vector, it is easily seen that [10]

$$d\underset{\sim}{n}_r/dr = \underset{\sim}{n}_\theta \qquad \text{and} \qquad d\underset{\sim}{n}_\theta/d\theta = -\underset{\sim}{n}_r \qquad \text{(A3)}$$

Then, by substituting from equation (A2) into (A1) and using equation (A3), ρ becomes

$$\rho = [r^2 + (dr/d\theta)^2]^{3/2}/[2(dr/d\theta)^2 + r^2 - rd^2r/d\theta^2] \qquad \text{(A4)}$$

Finally, by letting r be $R_m e^{m\theta}$ and by simplifying, ρ becomes

$$\rho = r(1 + m^2)^{1/2} \qquad \text{(A5)}$$

APPENDIX B

HYPERBOLOID - A SURFACE OF REVOLUTION

A hyperboloid is a "ruled" surface of revolution [11]. (That is, it can be developed by straight-line elements.) The equation of a hyperboloid is

$$z^2 = r^2 - 1 \qquad \text{or} \qquad z = \pm(r^2 - 1)^{1/2} \tag{B1}$$

where z is the axial coordinate and r is the radial coordinate.

Equations (23) and (24) can be put into the form of equation (B1) by the following substitution: Let

$$\left.\begin{aligned} \xi &= \hat{r}/R_c \sin \psi_m \\ \kappa_1 &= [V + (t_0/2)]\cot \theta \\ \kappa_2 &= [-V + (t_0/2)]\cot \theta \\ \zeta &= R_c \sin \psi_m \cot \theta \\ z_1 &= (z - \kappa_1)/\zeta \\ z_2 &= (z - \kappa_2)/\zeta \end{aligned}\right\} \tag{B2}$$

Then, by substituting the parameters defined by equation (B2), equations (23) and (24) take the form

$$z_1 = -(\xi^2 - 1)^{1/2} \tag{B3}$$

and

$$z_2 = (\xi^2 - 1)^{1/2} \tag{B4}$$

REFERENCES

1. Huston, R. L., and Coy, J. J., "Ideal Spiral Bevel Gears - A New Approach to Surface Geometry," Journal of Mechanical Design, Vol. 103, No. 1, Jan. 1981, pp. 127-133.

2. Litvin, F. L., and Gutman, Y., "Methods of Synthesis and Analysis for Hypoid Gear-Drives of 'Formate' and 'Helixform,' Parts 1, 2, and 3," Journal of Mechanical Design, Vol. 103, No. 1, Jan. 1981, pp. 83-113.

3. Litvin, F. L., and Gutman, Y., "A Method of Local Synthesis of Gears Grounded on the Connections Between the Principal and Geodetic Curvatures of Surfaces," Journal of Mechanical Design, Vol. 103, No. 1, Jan. 1981, pp. 114-125.

4. Litvin, F. L., "Relationships Between the Curvatures of Tooth Surfaces in Three-Dimensional Gear Systems," NASA TM-75130, 1977.

5. Krenzer, T. J., "The Effect of Cutter Radius on Spiral Bevel and Hypoid Tooth Contact Behavior," American Gear Manufacturers Association Semi-Annual Meeting, Washington, D.C., AGMA Paper No. 129.21, Oct. 1976.

6. Bonsignore, A. T., "The Effect of Cutter Diameter on Spiral Bevel Tooth Proportions," American Gear Manufacturers Association Semi-Annual Meeting, AGMA Paper No. 124.20, Washington, D.C., Oct. 1976.

7. Buckingham, E., Analytical Mechanics of Gears, Dover, New York, 1963, pp. 338-351.

8. Baxter, M. L., Jr., "Discussion on: 'Ideal Spiral Bevel Gears - A New Approach to Surface Geometry,'" Journal of Mechanical Design, Vol. 103, No. 1, Jan. 1981, p. 133.

9. Baxter, M. L., Jr., "Basic Theory of Gear-Tooth Action and Generation," Gear Handbook, D. W. Dudley, ed., McGraw Hill, New York, 1962, p. 1-16.

10. Kane, T. R., Analytical Elements of Mechanics, Vol. 2, Academic Press, New York, 1961, pp. 24, 41.

11. Lipschutz, M. M., Schaum's Outline of Theory and Problems of Differential Geometry, McGraw Hill Book Co., New York, 1969, p. 164.

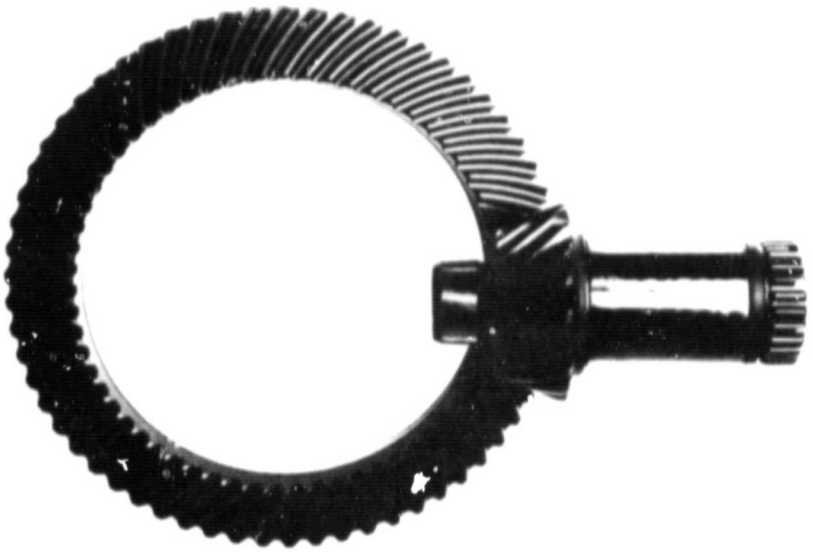

Figure 1. - Spiral-bevel gear and pinion.

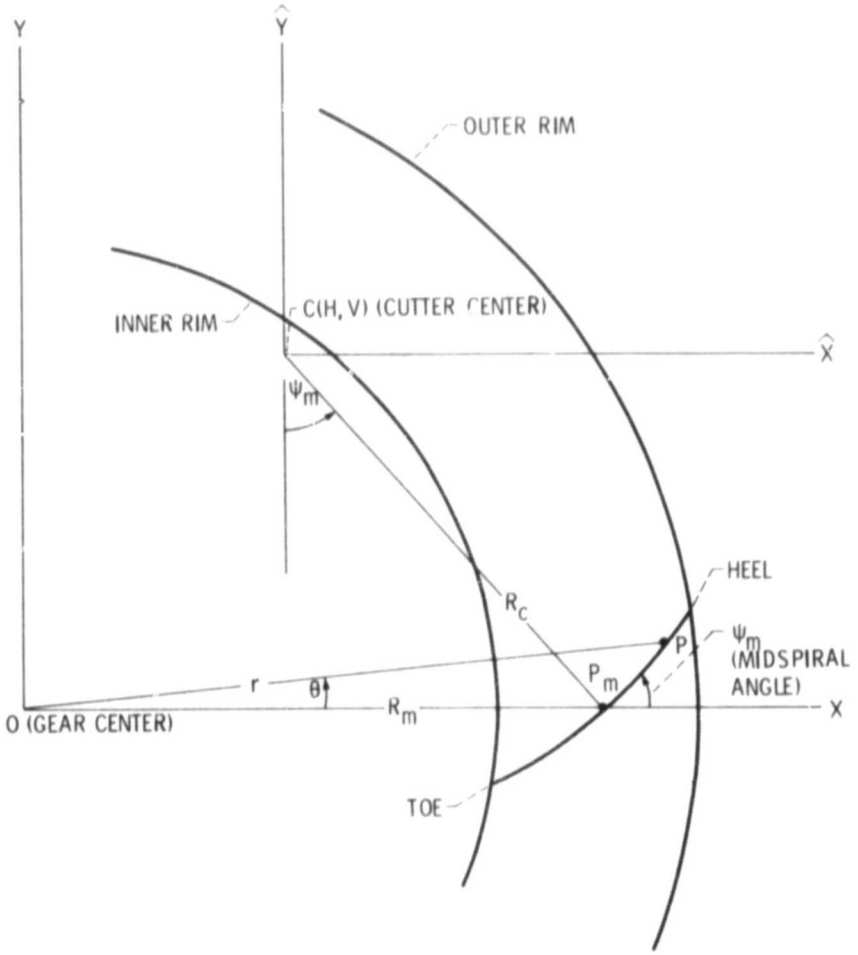

Figure 2. - Top view of circular-cut crown gear with centerline of typical tooth.

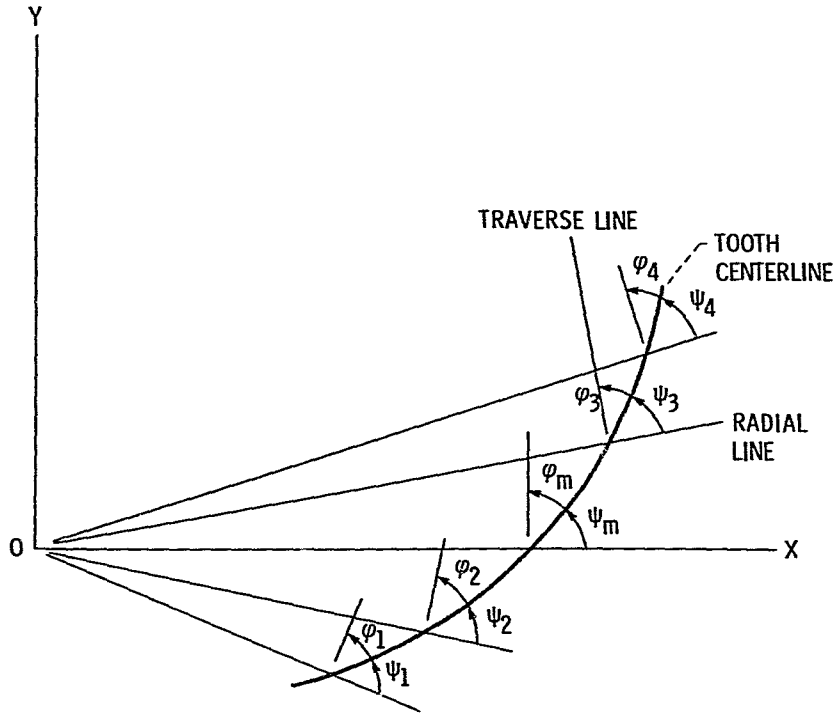

Figure 3. - Tooth centerline, radial line, and spiral angles.

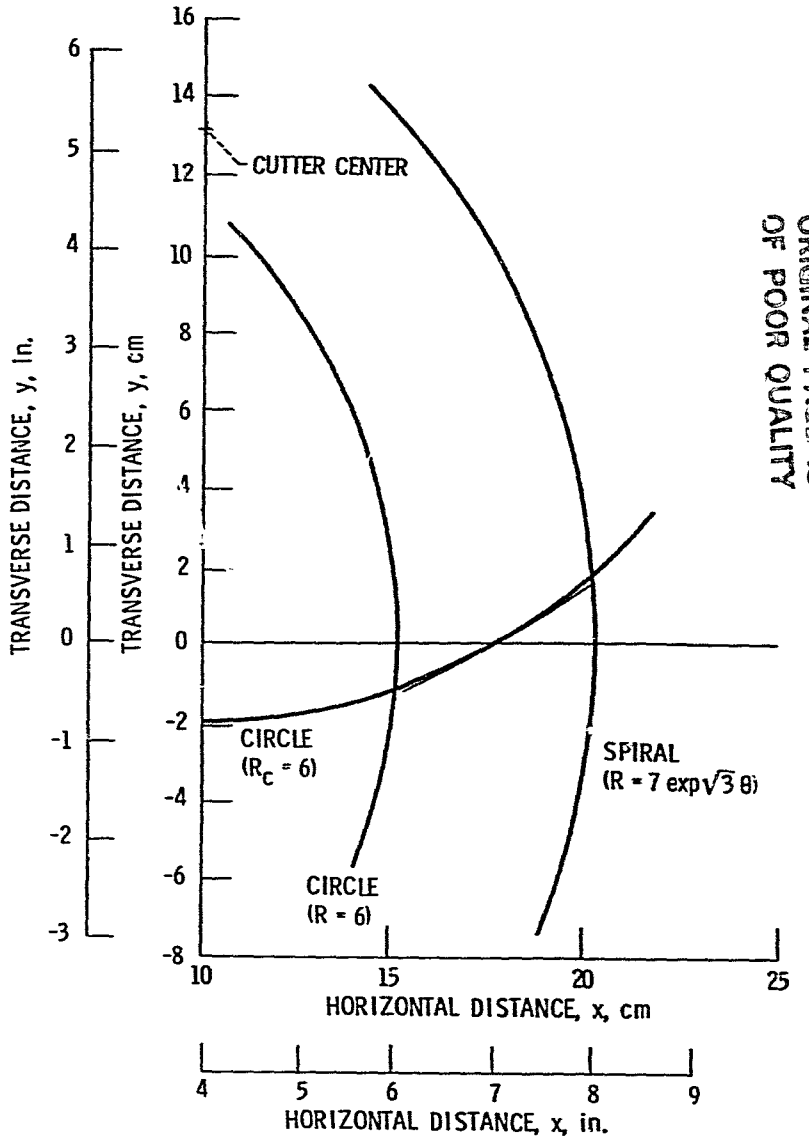

Figure 4. - Computer graph of crown gear, circular arc, and logarithmic spiral.

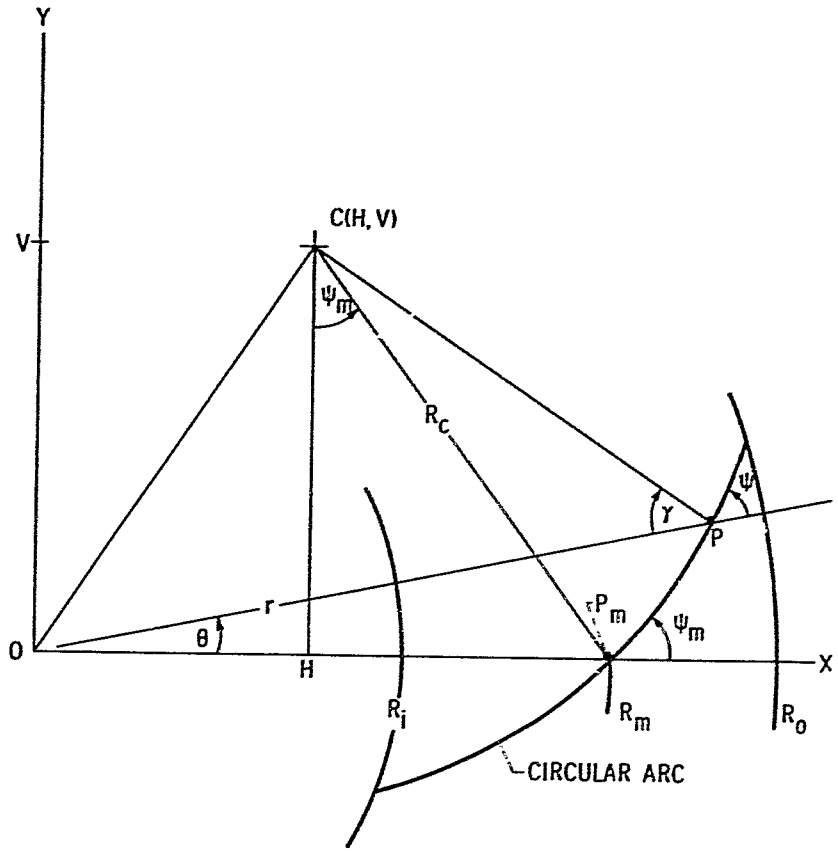

Figure 5. - Enlarged view of circular-arc tooth centerline.

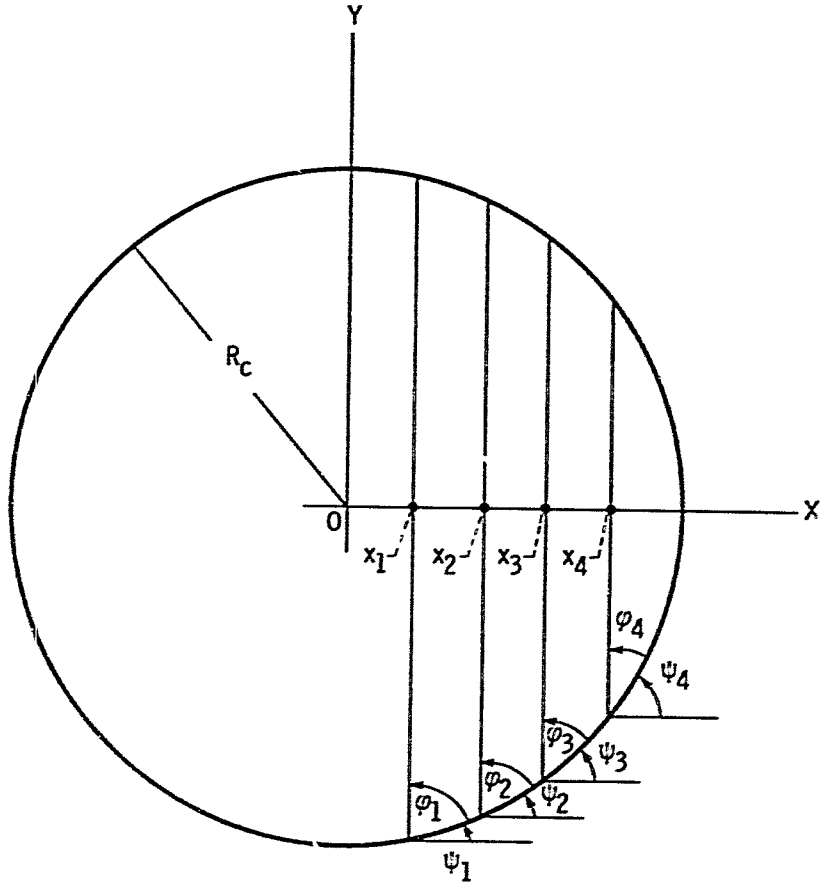

Figure 6. - Simulation of transverse angles by lines cutting a circle.

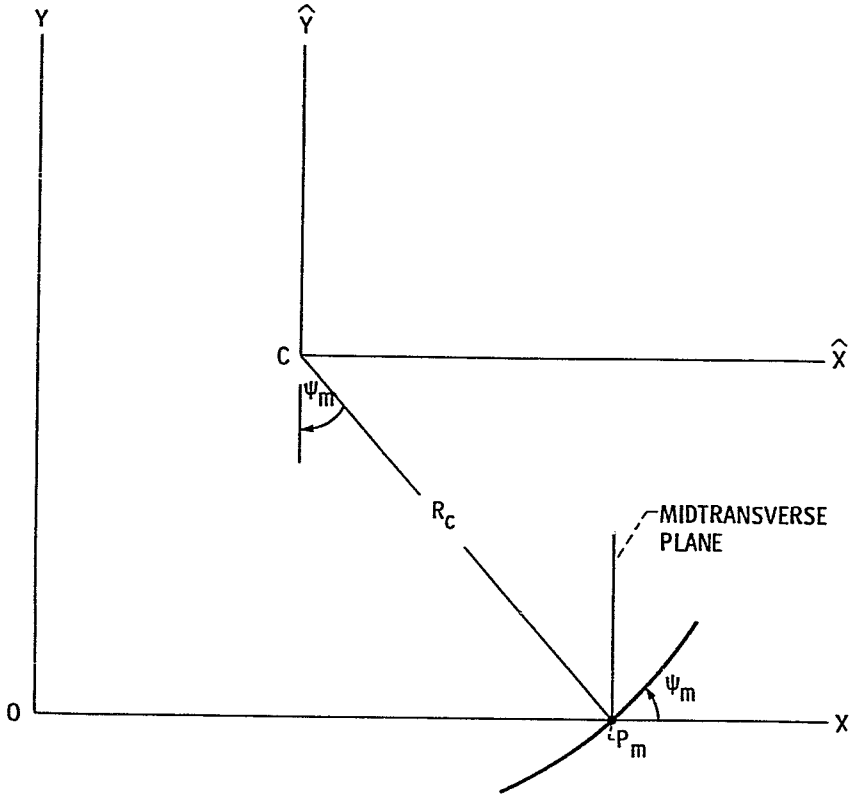

Figure 7. - Pitch plane of circular-cut crown gear.

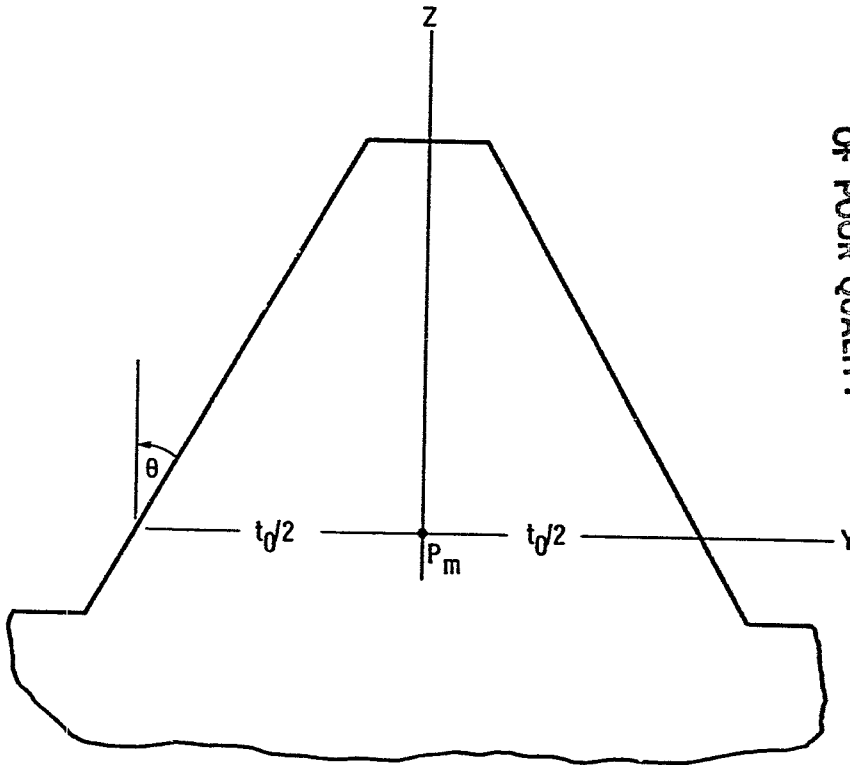

Figure 8. - Tooth profile of crown rack in midtransverse plane.

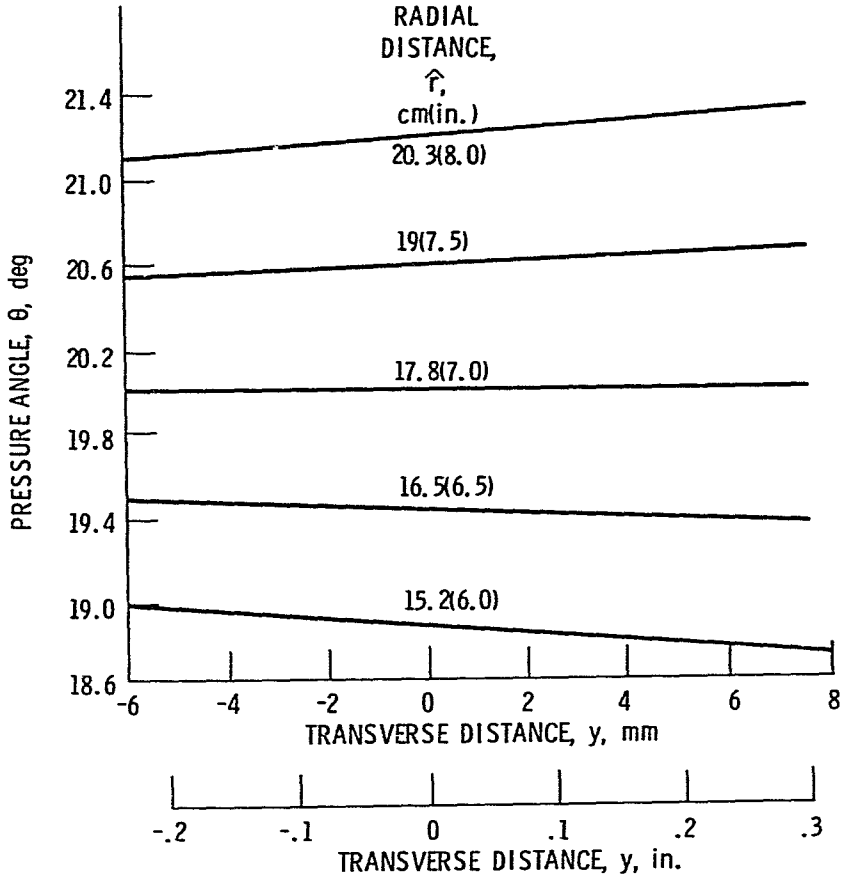

Figure 9. - Variation of pressure angle with transverse distance.

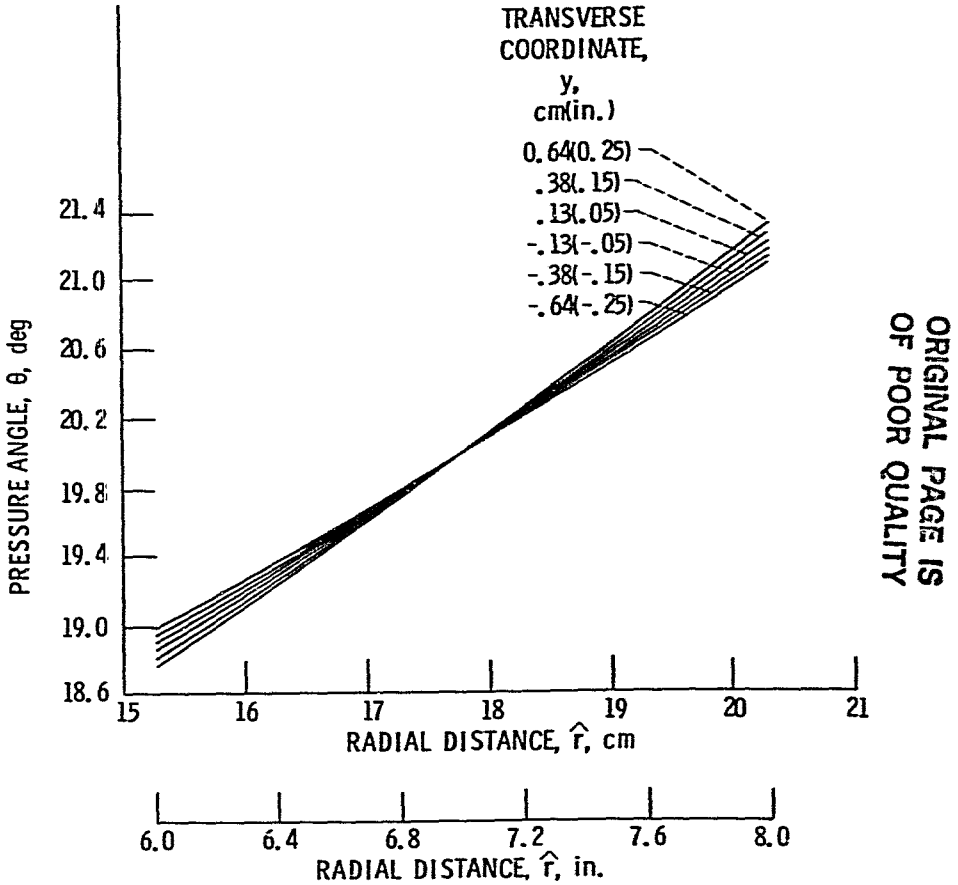

Figure 10. - Variation of pressure angle with radial distance.

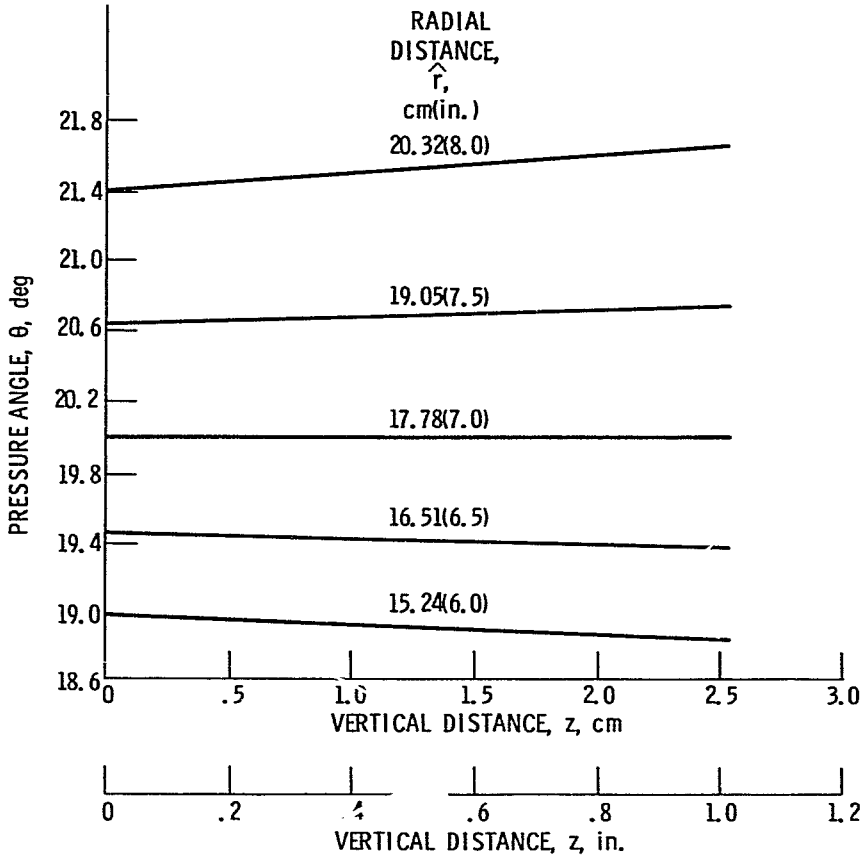

Figure 11. - Variation of pressure angle with vertical coordinate.

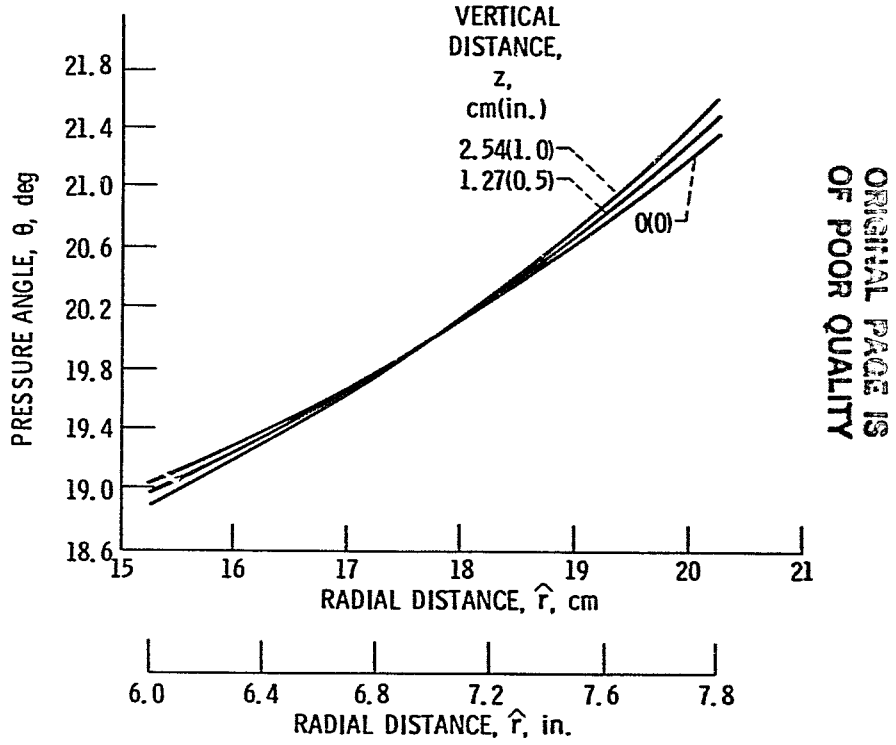

Figure 12. - Variation of pressure angle with radial distance.